

Syntheses and crystal structures of strained planar silacyclynes containing a diacetylene unit

Li Guo ^a, Joseph M. Hrabusa III ^a, Claire A. Tessier ^a, Wiley J. Youngs ^{a,*}, Robert Lattimer ^b

^a Department of Chemistry, The University of Akron, Akron, OH 44325-3601, USA

^b Advanced Technology Group, BF Goodrich, Brecksville, OH 44141-3289, USA

Received 8 May 1998

Dedicated to Professor Peter Jutzi on the occasion of his 60th birthday

Abstract

The synthesis and structural characterization of three silicon diacetylenic heterocyclines 1,1-diisopropyl-4,5:10,11-dibenzosilacyclotrideca-4,10 diene-2,6,8,12-tetrayne (**4**), 1,1-dimethyl-4,5:10,11-dibenzosilacyclotrideca-4,10-diene-2,6,8,12-tetrayne (**5**), and 1-methyl-1-*n*-octadecyl-4,5:10,11-dibenzosilacyclotrideca-4,10-diene-2,6,8,12-tetrayne (**6**) are reported. A dimer (**7**) and a cobalt complex (**9**) of **4** have also been characterized. Deprotonation of 1,4-di-(*o*-ethynylphenyl)butadiyne with two equivalents of *n*-BuLi resulted in the formation of the dianion. Addition of one equivalent of the appropriate dialkyldichlorosilane to a highly diluted THF solution of the dianion resulted in the formation of compounds **4**, **5**, **6** and **7**. These compounds were irradiated and were annealed. Comparisons to related compounds are made. © 1999 Elsevier Science S.A. All rights reserved.

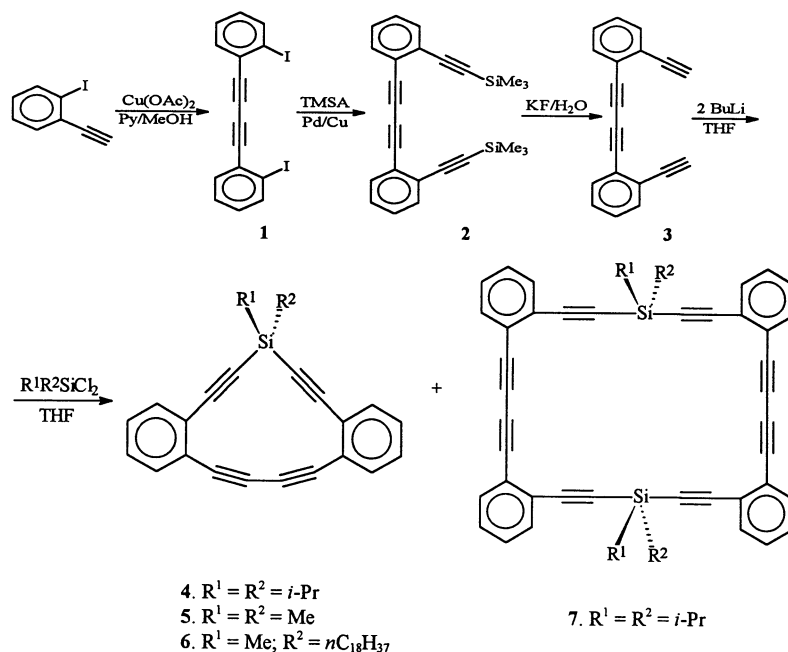
Keywords: Silicon; Diacetylene; Heterocycline; 1,4-Topological polymerization

1. Introduction

Solid state 1,4-topological polymerization of conjugated diacetylenes, first reported by Wegner in 1969 [1], has been a topic of considerable research interest. The resulting polymer chains are parallel to each other. The polymer crystals thus produced have optical, electrical and mechanical properties with pronounced anisotropy [2]. Extensive π -conjugation along the diacetylene backbones is responsible for their nonlinear optical (NLO) properties [3,4]. Polydiacetylenes are well known for their promising third-order nonlinear optical properties [5]. However, the synthesis of polydiacetylenes is not straightforward [6,7]. Most diacetylene monomers are composed of linear diacetylene rods with a variety of

substituents on either end [2]. As an offshoot of our studies on planar silacyclines [8] and continuing interest in diacetylenes [9], strained silacyclines which contain a diacetylene moiety have been synthesized. The strained nature of these diacetylenes could induce polymerization in the solid state. The introduction of the silyl group into such a system is of interest because silicon containing polymers have novel optical and electronic properties [10,11]. The incorporation of different substituents on silicon would be expected to alter the properties of this monomer and thus its polymer. Reported herein are the synthesis, structural characterization, spectroscopic results, and preliminary thermal stability studies of the strained silacycline–diacetylene compounds **4**, **5** and **6**, the silacycline–diacetylenic dimer **7**, and their precursor **3**. We also report the synthesis and structural characterization of **9**, a cobalt complex of **4**.

* Corresponding author.



Scheme 1.

2. Results and discussion

The synthetic route to **4**, **5** and **6** is outlined in Scheme 1. Glaser coupling of *o*-iodophenylacetylene with copper(II)acetate in pyridine/methanol at r.t. gave 1,4-di-*o*-iodophenylbutadiyne (**1**) in 90% isolated yield. Palladium–copper catalyzed coupling of trimethylsilylacetylene with 1,4-di-*o*-iodophenylbutadiyne gave 1,4-di-(*o*-trimethylsilylphenyl)butadiyne (**2**) in 90% yield. Compound **2** was readily desilylated with KF to form 1,4-di-(*o*-ethynylphenyl)butadiyne (**3**) in quantitative yield. The combination of 1,4-di-(*o*-ethynylphenyl)butadiyne in THF with 2 equivalents of freshly standardized *n*-butyl lithium resulted in a deep green solution. The mixture was then introduced into a highly dilute solution of dialkyldichlorosilane in THF to afford the desired products. The isolated yields for compound **4**, **5** and **6** are 32, 30 and 66%, respectively. High dilution (0.002 M) was used for the second step to avoid polymer formation. The cyclic dimer **7** was isolated in 13% yield as a crystalline solid. The cyclic dimers related to compounds **5** or **6** were not observed. Compounds **4**, **5**, **6** and **7** are white solids, very stable in air at room temperature and crystallize readily from a mixture of methylene chloride and hexane. The crystal structures of compounds **4**, **5** and **7** have been obtained.

Low temperature single-crystal X-ray crystallographic results reveal the structural details of compound **4** and compound **5** (Fig. 1). They have quite similar structures. The central pockets, which contain silicon and the alkynes (Si, C1 to C12), are planar in both compounds with deviations from planarity of

$\pm 0.0334 \text{ \AA}$ and $\pm 0.0467 \text{ \AA}$ for **4** and **5**, respectively. The maximum deviations from the planes (Si, C1 to C12) in **4** and **5** are the silicon atoms at -0.0633 and -0.1671 \AA , respectively. The diacetylene portions are bowed [12] with the four carbon atoms of the diacetylene (C5, C6, C7 and C8) deviating from linearity by an average of 8.1° (ranging from 6.0 to 12.1°) in **4** and 8.5° (ranging from 6.9 to 11.1°) in **5**. The angles at the silicon atom in both molecules are very close to the ideal tetrahedral angle, indicating that there is no angular strain on the silicon atoms. This differs from the analogous single alkyne cyclyne **8**, in which the internal $\equiv\text{C}-\text{Si}-\text{C}\equiv$ is 100.1° [8b]. The dialkyne moiety widens the internal angle of the silicon atom. The bond length of silicon to alkyne carbons is 1.840 \AA on average, compared to that of 1.822 \AA in **8**. The average bond length of all alkynes is 1.206 \AA for compound **4** and 1.198 \AA for compound **5**. Table 1 lists selected bond lengths and angles for compounds **4**, **5** and **9**.

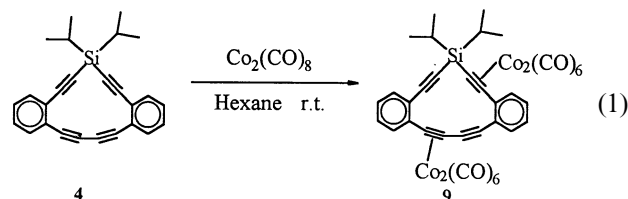
The structure of compound **7**, as shown by X-ray crystallography, consists of a 26-membered ring of pseudo-hexagonal geometry (Fig. 2). Compound **7** adopts a chair conformation as dictated by the tetrahedral geometry requirement of two silicon atoms as well as the spatial repulsion of four isopropyl groups. Both diacetylenes in **7** show small deviations from linearity with the $\text{C}\equiv\text{C}-\text{C}$ angles ranging from $\text{C4}-\text{C5}-\text{C6}$ $177.4(4)^\circ$ to $\text{C6}-\text{C7}-\text{C8}$ $179.4(4)^\circ$. The two opposing diacetylenes are 8.416 \AA (X1A to X1B) away from each other. The mean bond length of all eight alkynes is 1.199 \AA which corresponds to that in a normal alkyne bond. The valence angles of silicon $\equiv\text{C}-\text{Si}-\text{C}\equiv$

(104.0(2)° and 104.3(2)°) are smaller than tetrahedral values. The acetylene carbons adjacent to the silicon atoms are bent slightly inward with deviations from linearity ranging from 169.1(3)° at Si2–C13–C14 to 176.9(3)° at Si1–C24–C23. Similar results have been found in dodecamethyl(6)pericyclinosilane, (Me₂SiC≡C)₆, where C≡C–Si angles range from 174.8(5) to 176.7(6)° [13,14]. Selected bond lengths and angles of **7** are listed in Table 2.

Table 3 lists the IR (C≡C stretch), UV-vis, and ¹H-NMR in the aromatic region for compounds **4**, **5**, **6**, **7** and **8**. All compounds in comparison have very

similar coupling patterns for the aromatic protons in their ¹H-NMR and their UV-vis show an absorbance at similar wave numbers. In order to understand the UV-vis spectrum of the cyclic silane compounds **4**, **5** and **6**, it is useful to compare the spectra of these compounds to that of **8** [8b]. In **8**, there is no diacetylene in the heterocycle, instead a single alkyne replaces the diacetylenic moiety between the two benzo groups (Fig. 1). The long wavelength UV-vis absorption maxima of compounds **4**, **5** and **6** occur at ca. 366 nm, $\epsilon = 3.1 \times 10^4$ to 4.0×10^4 (Table 3), whereas the corresponding peak of **8** appears at 334 nm, $\epsilon = 3.2 \times 10^4$. This bathochromic shift of 32 nm in going from compound **8** to **4** reveals the enhancement of conjugation in compound **4** derived from the diacetylenic moiety. In other bent diacetylenes, it is believed that the bending distortion of the diacetylene is not responsible for the bathochromic shift [15,16]. The substantial bathochromic shift in **4** and **5** is probably due to homoconjugation rather than strain. This conclusion was drawn based on a strained cyclotetradeca-1,3-diyne [17] and its unstrained reference compound di-*tert*-butyl-1,3-butadiyne that share the same UV absorption maxima. The UV-vis spectrum of compound **7** shows only one strong peak at 240 nm. The long wavelength maximum in the spectrum of compound **7** appears only as a small shoulder at 354 nm of the peak at 240 nm. The weakness of the absorption is presumably due to the nonplanar nature of compound **7**, and the resulting lack of conjugation throughout the ring.

In order to make reactivity comparisons of mono- and diacetylenic heterocyclines, a cobalt complex, **9**, of ligand **4** was synthesized as described in Equation 1. Compound **4** was combined with an excess of dicobaltocarbonyl (2.4 equivalents) in 15 ml of hexane at room temperature and stirred overnight. Workup and crystallization from a solvent mixture of hexane and diethyl ether resulted in dark red crystals.



An X-ray crystal structure of complex **9** was obtained at low temperature. It crystallizes in the monoclinic space group *P*2₁/*c* with one molecule per asymmetric unit. The thermal ellipsoid labeling diagram of complex **9** is shown in Fig. 3. Fig. 4 shows the structure of the ligand moiety in the complex.

The crystal structure of complex **9** clearly reveals that one dicobalthexacarbonyl moiety is coordinated with one alkyne of the diacetylene and that the other dicobalthexacarbonyl moiety is coordinated to one

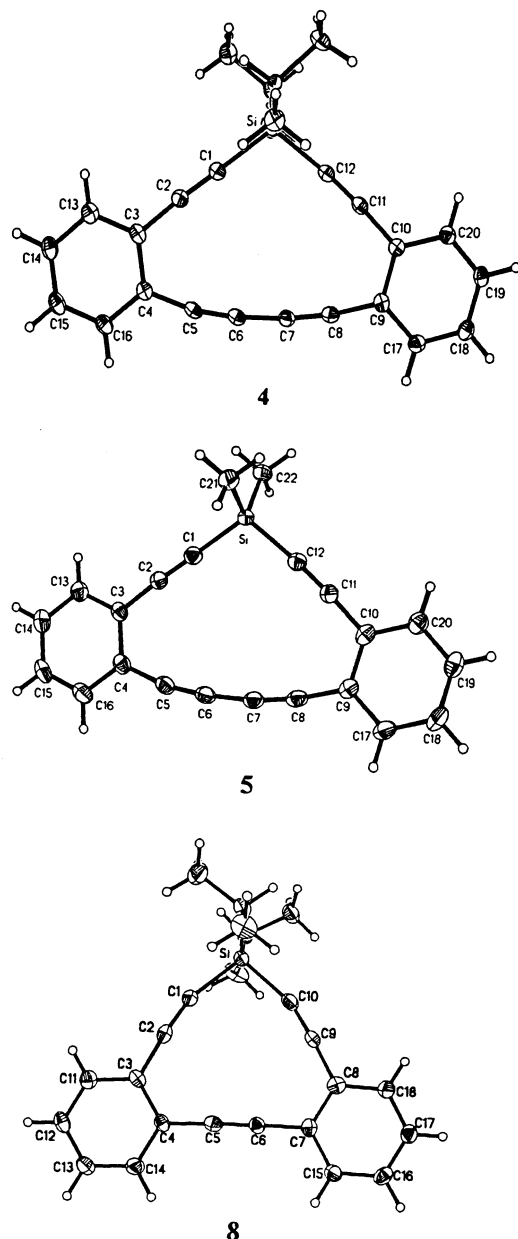


Fig. 1. Thermal ellipsoid plots of **4**, **5** and **8** drawn at 50% probability.

Table 1
Selected bond lengths (Å) and angles (°) for compounds **4**, **5** and **9**

Bond lengths	4	5	9	Bond angles	4	5	9
Si–C1	1.837(2)	1.826(2)	1.843(9)	C1–Si–C12	108.26(8)	107.13(10)	106.6(4)
Si–C12	1.842(2)	1.826(2)	1.855(9)	Si–C1–C2	178.2(2)	176.2(2)	146.2(7)
C1–C2	1.209(2)	1.201(3)	1.34(1)	C1–C2–C3	176.4(2)	177.0(2)	145.2(8)
C2–C3	1.440(2)	1.434(3)	1.45(1)	C2–C3–C4	119.2(2)	119.1(2)	123.2(8)
C4–C5	1.432(2)	1.412(3)	1.45(1)	C3–C4–C5	117.4(2)	118.3(2)	120.1(8)
C5–C6	1.203(3)	1.197(3)	1.20(1)	C4–C5–C6	167.9(2)	168.9(2)	169(1)
C6–C7	1.374(2)	1.364(3)	1.39(1)	C5–C6–C7	173.4(2)	173.1(2)	172(1)
C7–C8	1.204(2)	1.192(3)	1.35(1)	C6–C7–C8	174.0(2)	172.6(2)	152.3(9)
C8–C9	1.430(2)	1.420(3)	1.46(1)	C7–C8–C9	172.3(2)	171.4(2)	143.0(8)
C10–C11	1.443(2)	1.429(3)	1.46(1)	C8–C9–C10	118.3(2)	118.4(2)	123.5(8)
C11–C12	1.209(2)	1.201(3)	1.20(1)	C9–C10–C11	119.0(2)	119.4(2)	122.9(8)
C3–C4	1.419(2)	1.415(3)	1.44(1)	C10–C11–C12	175.2(2)	176.6(2)	173.3(9)
C9–C10	1.419(2)	1.416(3)	1.39(1)	C11–C12–Si	176.1(2)	173.4(2)	179.6(9)

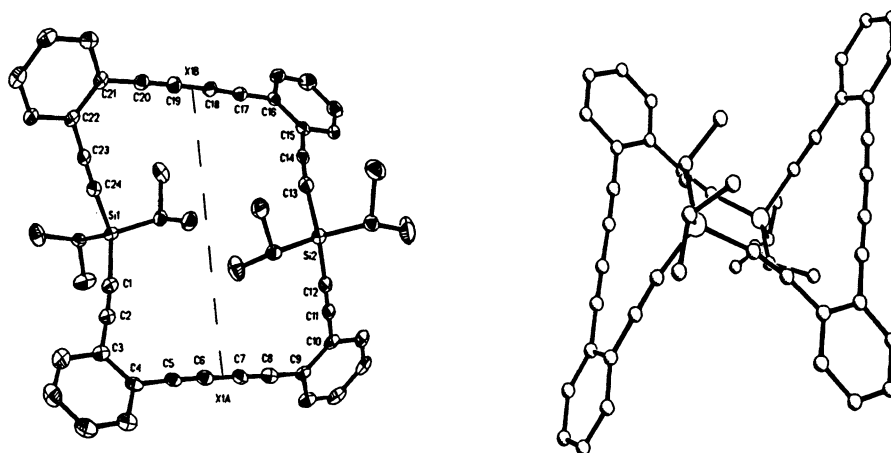


Fig. 2. Two views of the crystal structure of **7**. Hydrogen atoms are omitted for clarity. On the left is the thermal ellipsoid plot drawn at 50% probability. The chair conformation of **7** is shown on the right.

Table 2
Selected bond length (Å) and angles (°) for compound **7**

7							
Si1–C1	1.842(3)	C7–C8	1.196(6)	C1–Si1–C24	104.3(2)	Si2–C12–C11	174.4(3)
Si1–C24	1.833(4)	C11–C12	1.210(5)	C12–Si2–C13	104.0(2)	Si2–C1C–C14	169.1(3)
Si2–C12	1.833(4)	C13–C14	1.198(5)	Si1–C1–C2	169.9(3)	C17–C18–C19	178.3(4)
Si2–C13	1.844(3)	C17–C18	1.198(5)	C5–C6–C7	178.4(4)	C18–C19–C20	179.1(4)
C1–C2	1.198(4)	C19–C20	1.193(5)	C6–C7–C8	179.4(4)	Si1–C24–C23	176.9(3)
C5–C6	1.201(6)						

Table 3
Spectral data for compounds **4**, **5**, **6**, **7** and **8**

	IR $\nu(\text{C}\equiv\text{C})$ (cm^{-1})		UV-vis λ_{max} (nm) and ε ($\times 10^{-4}$)		$^1\text{H-NMR}$ of aromatic protons $\delta(\text{ppm})$ in C_6D_6		
4	2152 (s)	2211 (w)	366	4	7.25	6.97	6.64
5	2157 (s)	2209 (w)	364	3.8	7.28	6.97	6.64
6	2157 (s)	2211 (w)	366	3.1	7.30	6.99	6.64
7	2160 (s)	(w)	354	weak	7.47	7.20	7.09
8	2153 (s)		334	3.2	7.44	7.34	6.77

alkyne adjacent to silicon. After reviewing the cobalt chemistry of analogous silicon cyclyne ligands $\text{SiPh}_2(\text{OBET})$ and $\text{Ge}(\text{OBET})_2$ [18], we have concluded that dicobalthexacarbonyl selectively complexes strained alkynes. In the series of compounds (**4**, **5** and **6**) in which diacetylene is incorporated in the silicon cyclyne ring, the most strained alkyne is one of the diacetylenes. Therefore, one alkyne in the diacetylene in ligand **4** is coordinated with dicobalthexacarbonyl. Apparently, this complexation shields the second alkyne in the diacetylene from reacting with dicobaltoctacarbonyl because it is part of a ring. The rest of the dicobaltoctacarbonyl reacted with one of the alkynes next to silicon atom. The ^1H - and the ^{13}C -NMR spectral results show that the bulk sample contains one complex and the number of peaks is consistent with the X-ray structure. There are reports that both alkynes in bis-trimethylsilylbutadiyne react with an excess of dicobaltoctacarbonyl [19]. Pannell reported that either one or both of the alkynes in bis-trimethylsilylbutadiyne coordinated with dicobalt carbonyl. There are at least two reported X-ray crystal structures of complexes in which both alkynes in a diacetylene moiety are coordi-

nated to dicobalthexacarbonyl [20,21]. Corriu reported the high yield reactions of poly[(silylene)diacetylenes] and its analogs with dicobaltoctacarbonyl to form complexes in which only one of the alkynes in the diacetylene moiety was coordinated with cobalt carbonyl [10].

Selected bond lengths and angles for complex **9** are listed with its free ligand **4** in Table 1. The coordinated alkyne bond lengths are 1.34(2) and 1.33(2) Å for $\text{C1}\equiv\text{C2}$ and $\text{C7}\equiv\text{C8}$, respectively. The bond length of $\text{C1}-\text{Si}$ is 1.85(2) Å, whereas $\text{C12}-\text{Si}$ which is uncoordinated to cobalt is 1.86(2) Å. They are not significantly longer than those in the free ligand, which is 1.840(2) Å on average. Among the four alkyne carbons in the diacetylene moiety of free ligand, the smallest angle is $167.9(2)^\circ$ at $\text{C4}-\text{C5}-\text{C6}$. This angle $\text{C4}-\text{C5}-\text{C6}$ becomes $170.9(14)^\circ$ upon complexation of the adjacent alkyne with dicobalthexacarbonyl. Among the four coordinated alkyne carbons, the average value is $147.2(28)^\circ$ ranging from $144.1(12)^\circ$ at C2 to $151.5(14)^\circ$ at C7 . Fig. 4 demonstrates that the planarity of the central frame is dramatically distorted at $\text{C1}\equiv\text{C2}$, but not at $\text{C7}\equiv\text{C8}$. This distortion is also observed in $\text{SiPh}_2(\text{OBET})(\text{Co}_2(\text{CO})_6)_2$ and $\text{Ge}(\text{OBET})_2(\text{Co}_2(\text{CO})_6)_2$. Ortho(bisethynyl)tolane (OBET) is similar to compound **3** but has only one alkyne between the benzo groups instead of a diacetylenic moiety. Unlike these two cobalt complexes, the inner angle of silicon, $\text{C1}-\text{Si}-\text{C12}$, is decreased from $108.26(28)^\circ$ in the free ligand **4** to $105.8(6)^\circ$ in its complex **9**. Crystal and data collection parameters for all the diacetylenic heterocyclynes are listed in Table 4.

It is well known that 1,3-butadiynes undergo topological polymerization in their crystalline states on exposure to heat, UV light or γ radiation. The crystal of a monomer 1,3-butadiyne acts as a preformed lattice for the polymer crystal. The monomers will polymerize if the diyne 'rods' are stacked parallel to each other in their crystal structures [2]. During the polymerization, successive diyne molecules tilt toward the stacking axis so that the terminal acetylenic carbons of adjacent molecules move within bonding range (Fig. 5). Reactivities are dependent on the stacking pattern of the monomers in the crystal. If s is defined as the perpendicular distance between two adjacent diyne rods, d is the distance between the centers of two adjacent alkynes, and r is the angle between the diacetylene rod and the stacking axis, then $s = d (\sin r)$. Baughman [22] and Wegner [23] specified that for significant reactivity, s should be about 3.4–4.0 Å and r about 45° . Huntsman [2] has examined monomeric diacetylenes and found that reactive diynes in general satisfy these requirements, but that some diacetylenes still showed reactivity toward polymerization when their packing parameters deviated from the expected limits. The outer limits are observed as $r = 41\text{--}60^\circ$, $d = 4.35\text{--}5.34$ Å and $s = 3.94\text{--}$

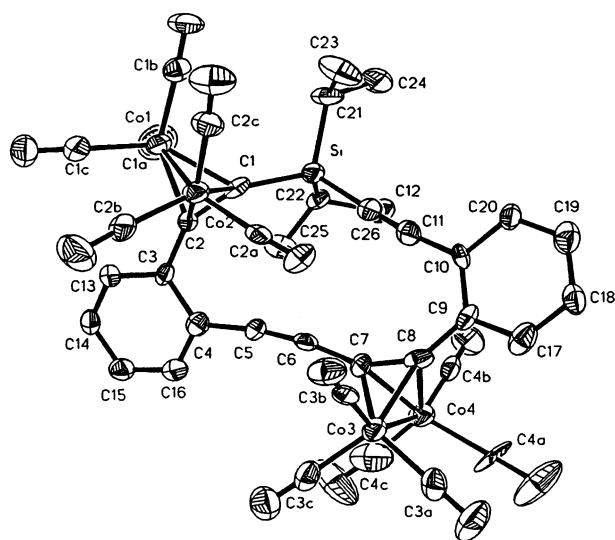


Fig. 3. Molecular structure of complex **9** with thermal ellipsoids drawn at 50% probability. Hydrogen atoms are omitted for clarity.

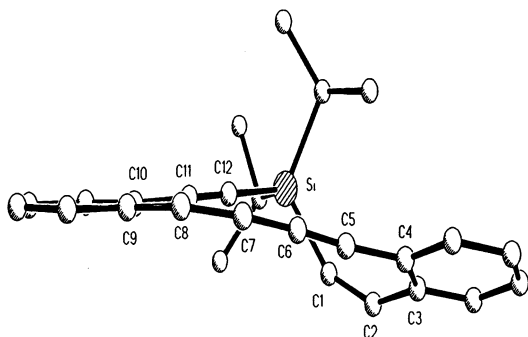


Fig. 4. The side view of the ligand **4** in complex **9**.

Table 4

Crystal and data collection parameters for compounds **3**, **4**, **5**, **7** and **9**

Compound	3	4	5	7	9
Formula	C ₂₀ H ₁₀	C ₂₆ H ₂₂ Si	C ₂₂ H ₁₄ Si	C ₅₂ H ₄₄ Si ₂	C ₃₈ H ₂₂ Co ₄ O ₁₂ Si
Molecular weight	250.28	362.53	306.42	725.1	934.37
Cryst. color	Colorless	Colorless	Colorless	Colorless	Deep red
Cryst size (mm)	0.15 0.25 0.40	0.30 0.40 0.40	0.20 0.40 0.60	0.25 0.40 0.40	0.30 0.40 0.60
Space group	<i>P</i> $\bar{1}$	<i>P</i> 2 ₁ / <i>c</i>	<i>P</i> 2 ₁ / <i>c</i>	<i>P</i> 2 ₁ / <i>c</i>	<i>P</i> 2 ₁ / <i>c</i>
<i>a</i> (Å)	7.264(1)	14.279(2)	5.272(1)	20.116(4)	19.67(2)
<i>b</i> (Å)	7.378(1)	9.1397(13)	20.239(4)	11.461(2)	12.478(8)
<i>c</i> (Å)	7.391(1)	15.661(2)	15.180(3)	18.532(4)	17.45(2)
α (°)	74.93(3)	90	90	90	90
β (°)	74.03(3)	91.212(10)	90.89(3)	100.75(3)	115.39(6)
γ (°)	64.33(3)	90	90	90	90
<i>V</i> (Å ³)	338.68(8)	2043.4(5)	1619.5(5)	4197.6(14)	3869(6)
ρ_{calcd} (g cm ⁻³)	1.227	1.178	1.257	1.147	1.604
<i>Z</i>	1	4	4	4	4
<i>T</i> (K)	141	100	147	100	140
Reflections (indep.)	1092	3591	2627	7380	6754
Reflections (obs.)	830	2977	2109	4298	3292
Parameters refined	91	244	208	491	496
<i>R</i> 1 (%)	4.72(<i>I</i> > 2 σ (<i>I</i>))	3.63(<i>I</i> > 2 σ (<i>I</i>))	4.46(<i>I</i> > 2 σ (<i>I</i>))	5.65(<i>F</i> > 4 σ (<i>F</i>))	5.68(<i>I</i> > 2 σ (<i>I</i>))
<i>R</i> 2[%](all data)	6.84	4.95	5.971	1.21	1.16

3.50 Å among the examples in the paper. Due to the difficulties of actually running the polymerizations, Paley et al. [6] reported that computer modeling could predict the potential polymerizability of monomers. Statistically, all of the compounds which are known to polymerize readily in the solid state tend to have $d = 5\text{--}6.5$ Å and $r = 45\text{--}67^\circ$. In conclusion, no matter what the packing parameters are for the topological polymerization to occur, the overall orientation should favor new bond formation between two adjacent diacetylenes in the process of 1,4-addition.

The thermal ellipsoid labeling diagram of compound **3** is shown in Fig. 6. Selected bond lengths and angles for compound **3** are listed in Table 5. Packing diagrams of compounds **3**, **4** and **5** are displayed in Fig. 7. They are packed parallel to each other in their solid state for all three crystal structures. Their packing parameter calculations are shown in Fig. 8 with results listed in Table 6. The perpendicular distance s for compound **4** is within the optimum limit. However the stacking distance $d = 9.14$ Å between the monomers in the array and the angle $r = 23.3^\circ$ between the diacetylene rods

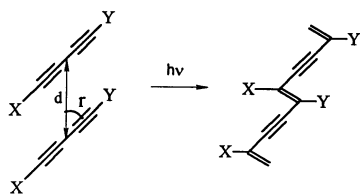


Fig. 5. 1,4-Addition of diacetylene: d is the distance between the centers of two alkynes; r is the angle between the diacetylene rod and the stacking axis and s is the perpendicular distance between two adjacent diacetylene rods.

and the stacking axis fall outside of the limits derived from calculations for diacetylenes that are reactive in the solid state. The packing diagrams suggest that intermolecular spatial repulsions of isopropyl groups prevent the diyne units from moving into favorable bonding orientations. With this in mind, we synthesized its analog **5** in which smaller methyl groups are attached to the silicon atom instead of isopropyl groups. Its packing parameters indeed exhibit adjacent diacetylene rods stacked closer to each other having $d = 5.27$ Å. The angle $r = 42.9^\circ$ is much more favorable than that of compound **4**. Even though compound **3**

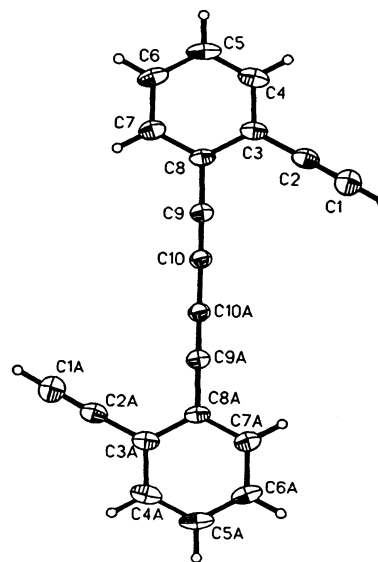


Fig. 6. Thermal ellipsoid plot of **3** drawn at 50% probability.

Table 5
Selected bond length (Å) and angles (°) for compound 3

3			
C1–C2	1.184(3)	C1–C2–C3	178.4(2)
C2–C3	1.430(3)	C2–C3–C8	120.3(2)
C3–C8	1.421(3)	C3–C8–C9	120.1(2)
C8–C9	1.431(3)	C8–C9–C10	179.4(2)
C9–C10	1.204(3)	C9–C10–C10A	179.3(3)
C10–C10A	1.370(4)		

has all the stacking parameters outside the optimum limit, it is the most unstable species of all. At room temperature its crystals gradually turn from colorless to dark brown on exposure to light. Compound 3 is stable when it is kept in a solution of hexane or methylene chloride in the dark.

Diacetylene polymerization can be induced by exposure to ultraviolet or X-ray radiation or heat annealing. To induce the 1,4-addition polymerization of compounds 5 and 3, their colorless crystals were placed on a watch glass and irradiated with a medium pressure mercury lamp for 4 days. While irradiating, the crystals of 5 turned brown and those of 3 turned metallic black. In many of the reports the polymer itself was not characterized, and the development of a deep red or blue color upon heating or irradiation serves as the evidence for the occurrence of the polymerization [2].

The $^1\text{H-NMR}$ of the brown irradiated 5 showed that it was principally the unreacted monomer, and the low temperature X-ray diffraction results of radiated crystals of 3 revealed that it was principally the same as its starting monomer. This indicates that the polymerization is only occurring at the surface with these compounds.

The thermal behavior of compounds 3, 4, 5 and 6 in the solid state has been studied by differential scanning calorimetry (DSC) and thermogravimetric analysis (TGA). The DSC and TGA of compound 4 show a large exothermic transition and 10% weight loss at 160°C. An exothermic transition for compound 5 occurs at 125° with a 10% weight loss. Due to the poor solubility of these annealed compounds, they have not yet been characterized. Compound 6 melts at 71°C and has a exothermic transition at 132°C without weight loss until the temperature reaches 390°C. Compound 3 exploded to form a black powder in the process of measurements. It has a exothermic peak at about 136°C and its weight loss is about 35%.

2.1. Experimental procedure

2.1.1. Materials

All chemicals were purchased from Aldrich Chemical and used as received unless otherwise stated. Solvents for reactions were dried and distilled before use. Tetrahydrofuran (THF) was predried with sodium hydroxide and distilled over sodium benzophenone ketyl to which a small amount of tetraethylene glycol dimethylether was added. All the dichlorosilanes were purchased from Gelest. Dimethyldichlorosilane and diisopropyldichlorosilane were treated with anhydrous potassium carbonate for at least a day and distilled from this reagent before use. Methyl-*n*-octadecyldichlorosilane was used after being pumped on under vacuum. *n*-Butyllithium in hexane (1.6 M) was purchased from Aldrich and was freshly standardized with diphenylacetic acid before use [24]. *o*-Iodophenylacetylene was synthesized by standard procedures [25]. All reactions were carried out under nitrogen using standard Schlenk techniques unless otherwise noted [26,27].

1,4-Di-(*o*-iodophenyl)butadiyne (1): *o*-Iodophenylacetylene (16 g, 70.2 mmol) was added to a mixture of pyridine (350 ml), methanol (350 ml) and cupric acetate (331.9 g, 175.5 mmol) and stirred for 1 day. Ice and diethylether followed by a mixture of sulfuric acid and ice were added to the mixture. The water layer was extracted with ether, and the combined ether extracts were washed with dilute sulfuric acid, water, and sodium carbonate solution, and dried over magnesium sulfate. Removal of the volatiles and recrystallization from hexane gave 1 as a white solid product (14 g) in 90% yield. $^1\text{H-NMR}$ (300 MHz, CDCl_3) δ 7.84 (d, 2H),

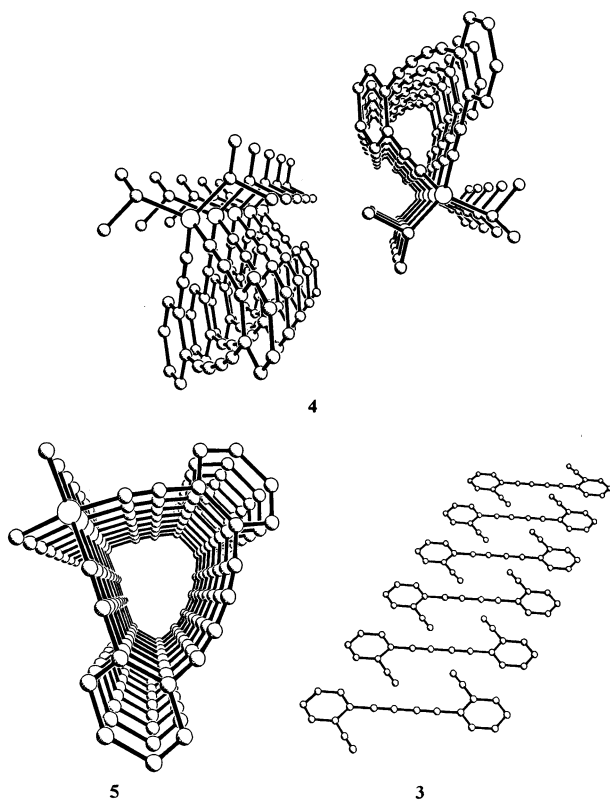


Fig. 7. Stacking pattern of compounds 3, 4 and 5.

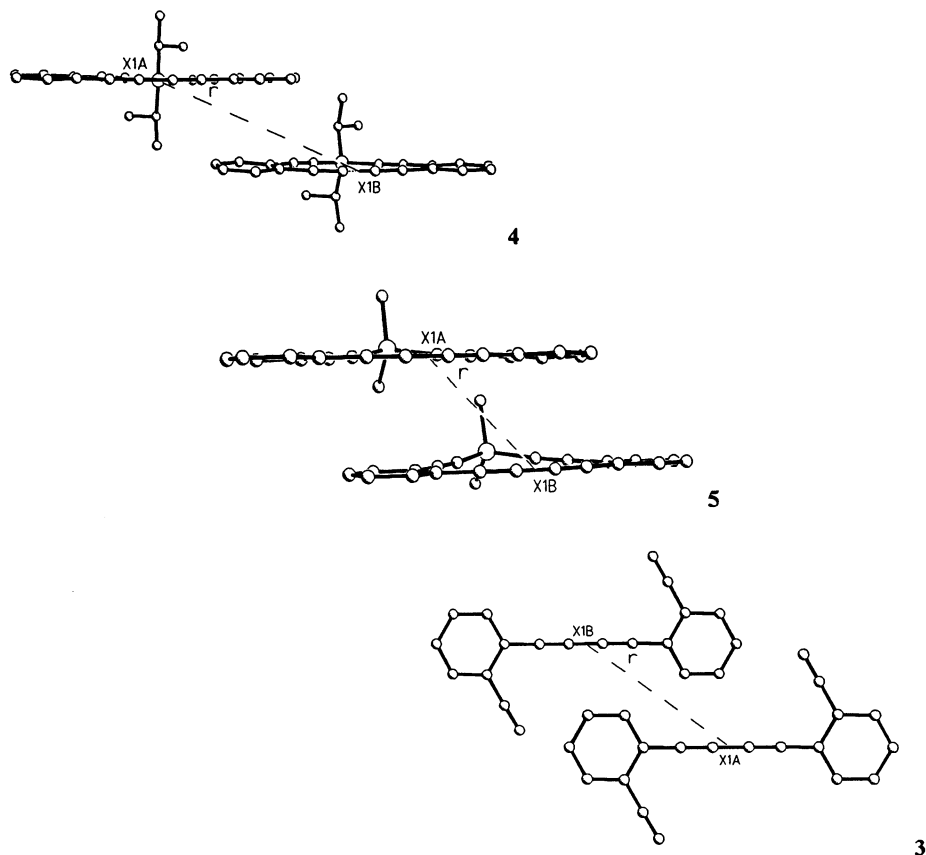


Fig. 8. Packing parameter calculations of compounds **4**, **5** and **3**.

7.54 (d, 2H), 7.31 (t, 2H), 7.04 (t, 2H); ^{13}C -NMR (75 MHz, C_6D_6) δ 138.8, 133.9, 130.3, 128.5, 127.8, 100.9, 84.3, 77.1; IR ($\text{C}\equiv\text{C}$ stretch) $2212\text{ cm}^{-1}(\text{s})$.

1,4-Di-(*o*-trimethylsilylethynylphenyl)butadiyne (2): Excess trimethylsilylacetylene (TMSA) was added to 1,4-di-*o*-iodophenylbutadiyne (6 g, 13.2 mmol), bis(benzonitrile)dichloropalladium(II) (0.506 g, 1.32 mmol), copper(I) iodide (0.251 g, 1.32 mmol), and triphenylphosphine (0.693 g, 2.64 mmol) in 50 ml of diisopropylamine and 150 ml benzene. After stirring for 12 h the mixture was filtered, the solvent removed under reduced pressure and the residue chromatographed on silica gel with hexane to afford **2** in 90% yield. ^1H -NMR (300 MHz, CDCl_3) δ 7.46 (m, 4H), 7.26 (m, 4H), 0.279 (s, 18H); ^{13}C -NMR (75 MHz, CDCl_3) δ 132.8, 132.1, 128.9, 128.4, 127.1, 125.3, 103.2, 100.0, 81.2, 78.1, 0.2. Anal. Calc. for $\text{Si}_2\text{C}_{26}\text{H}_{22}$: C 79.13%; H 6.64%; found C 79.20% H 6.59%; IR ($\text{C}\equiv\text{C}$ stretch) $2158\text{ cm}^{-1}(\text{s})$.

1,4-Di-(*o*-ethynylphenyl)butadiyne (3): 1,4-Di-(*o*-trimethylsilylethynylphenyl)butadiyne (0.651 g, 1.65 mmol), KF (0.274 g, 4.71 mmol), and water (0.17 ml, 9.41 mmol) were stirred in THF/MeOH (10/40 ml) at r.t. for 12 h. Extraction with CH_2Cl_2 , drying over magnesium sulfate and removal of solvent gave compound **3** in (97% yield). 1,4-Di-(*o*-ethynylphenyl)buta-

diyne melts at 120°C , but it explodes at ca. 125°C and turns into a black powder. ^1H -NMR (300 MHz, CDCl_3) δ 7.52 (m, 4H), 7.31 (m, 4H), 3.37 (s, 2H); ^{13}C -NMR (75 MHz, CDCl_3) δ 133.4, 133.0, 129.2, 128.9, 125.9, 125.2, 82.0, 81.8, 81.0, 72.8; IR ($\text{C}\equiv\text{C}$ stretch) 2252, 2214, 2158, 2140, $2109\text{ cm}^{-1}(\text{s})$.

2.2. General procedure for the synthesis of silacyclynes

2.2.1. Synthesis of 1,1-diisopropyl-4,5:10,11dibenzosilacyclotrideca-4,10 diene-2,6,8,12-tetrayne (**4**) and its dimer (**7**)

To a 100 ml flask charged with 1,4-di-(*o*-ethynylphenyl)butadiyne⁹ (300 mg, 1.2 mmol) in 40 ml of THF was added *n*-butyl lithium (1.37 ml, 2.4 mmol). The solution turned a deep green immediately. After 4 h, the mixture was transferred by cannula into a solu-

Table 6
Packing parameters of compounds **3**, **4** and **5**

	4	5	3
s (Å)	3.62	3.59	4.71
r (°)	23.3	42.9	39.6
d (X1A–X1B) (Å)	9.14	5.27	7.39

tion of diisopropyldichlorosilane (222.2 mg, 1.2 mmol) in 560 ml of THF. After stirring at 70°C for 12 h the reaction mixture was opened to air and worked up by removal of the volatiles at reduced pressure, extraction with $\text{CH}_2\text{Cl}_2/\text{H}_2\text{O}$, and drying of the organic phase over magnesium sulfate. The volatiles were removed under vacuum. Chromatography on silica gel eluting with hexane gave 32% yield of compound **4** and 13% yield of its cyclic dimer **7** as white solids. Crystals suitable for X-ray diffraction were grown from a hexane and methylene chloride mixture by slow evaporation of solvents. Data for compound **4**: $^1\text{H-NMR}$ (300 MHz, C_6D_6) δ 7.25 (d, 2H), 6.97 (d, 2H), 6.64 (pentet, 4H), 1.30 (d, 12H), 1.26 to 1.14 (m, 2H); $^{13}\text{C-NMR}$ (75 MHz, C_6D_6) δ 131.9, 130.2, 130.1, 129.2, 128.9, 126.9, 106.1, 94.9, 85.8, 81.9, 18.4, 13.0. FDMS, m/z 362 (M^+); Anal. Calc. for $\text{SiC}_{26}\text{H}_{22}$: C 86.14%; H 6.12%; found C 79.78% (the sample burned at 980°C when being measured) H 6.81%; IR ($\text{C}\equiv\text{C}$ stretch) 2152 $\text{cm}^{-1}(\text{s})$ and 2212 $\text{cm}^{-1}(\text{w})$. Data for compound **7**: $^1\text{H-NMR}$ (300 MHz, C_6D_6) δ 7.47 (d, 4H), 7.20 (m, 8H), 7.09 (t, 4H), 1.22 (d, 24H), 1.20 (m, buried under Me peaks); $^{13}\text{C-NMR}$ (75 MHz, CDCl_3) δ 132.9, 132.5, 128.4, 128.4, 126.6, 125.5, 104.8, 93.3, 81.1, 78.5, 18.0, 12.7. FDMS, m/z 724 (M^+); Anal. Calc. for $\text{Si}_2\text{C}_{52}\text{H}_{44}$: C 86.14%; H 6.12% found C 85.30% H 6.28%; IR: ν ($\text{C}\equiv\text{C}$) 2160 $\text{cm}^{-1}(\text{s})$.

2.2.2. Synthesis of 1,1-dimethyl-4,5:10,11-dibenzosilacyclotrideca-4,10-diene-2,6,8,12-tetrayne (**5**)

Using the procedure described for **4** above 1,4-di-*o*-ethynylphenylbutadiyne (250 mg, 1 mmol), two molar equivalents of *n*-butyl lithium (1.31 ml, 2 mmol), dimethyldichlorosilane (129.1 mg, 1.0 mmol) and 500 ml THF were used to prepare compound **5**. Chromatography on silica gel eluting with hexane/methylene chloride (8:1) gave 30% yield of compound **5** as a white solid. $^1\text{H-NMR}$ (300 MHz, C_6D_6) δ 7.28 (d, 2H), 6.97 (d, 2H), 6.64 (pentet, 4H), 0.397 (s, 6H), $^{13}\text{C-NMR}$ (300 MHz, C_6D_6) δ 131.6, 129.8, 129.7, 128.9, 128.6, 126.2, 104.2, 97.3, 85.6, 81.5, –0.4. $^{13}\text{C-NMR}$ (75 MHz, CDCl_3) δ 131.7, 129.7, 129.4, 129.0, 128.8, 125.9, 103.6, 96.9, 85.1, 80.6, –0.1; FDMS, m/z 306 (M^+); Anal. Calc. for $\text{SiC}_{22}\text{H}_{14}$: C 86.3%; H 4.6%; Found C 83.56% H 4.67%; IR ($\text{C}\equiv\text{C}$ stretch) 2157 $\text{cm}^{-1}(\text{s})$ and 2209 $\text{cm}^{-1}(\text{w})$.

2.2.3. Synthesis of 1-methyl-1-*n*-octadecyl-4,5:10,11-dibenzosilacyclotrideca-4,10-diene-2,6,8,12-tetrayne (**6**)

Using the procedure described for **4** above 1, 4-di-*o*-ethynylphenylbutadiyne (375 mg, 1.5 mmol), two equivalents of *n*-butyllithium (1.65 ml, 3 mmol), methyl-*n*-octadecyldichlorosilane (551.3 mg, 1.5 mmol) and a total of 750 ml of THF were used in the synthesis of **6**. Compound **6** was isolated in 66% yield as white

long needle like crystals. $^1\text{H-NMR}$ (300 MHz, C_6D_6) δ 7.30 (d, 2H), 6.99 (d, 2H), 6.64 (multiplet, 4H), 1.72 (m, 2H), 1.30 (d, 30H), 92 (m, 5H), 0.46 (s, 3H); $^{13}\text{C-NMR}$ (75 MHz, C_6D_6) δ 131.5, 129.8, 129.8, 128.9, 128.6, 126.2, 104.6, 96.8, 85.6, 81.5, 33.4, 32.3, 30.2, 30.2 (these last two peaks are very wide), 30.1, 30.1, 29.8, 29.7, 24.2, 23.1, 16.0, 14.4, –1.8; $^1\text{H}\{^{29}\text{Si}\}\text{NMR}$ (60 MHz, C_6D_6) δ –36.2. FDMS, m/z 544 (M^+), 272 (M^{++}); Anal. Calc. for $\text{SiC}_{39}\text{H}_{48}$: C 85.97%; H 8.88%; found C 79.89% H 8.79%; IR ($\text{C}\equiv\text{C}$ stretch) 2157 $\text{cm}^{-1}(\text{s})$ and 2211 $\text{cm}^{-1}(\text{w})$.

2.2.4. Synthesis of **9**, a cobalt complex of **4**

To a solution of **4** (65mg, 0.179 mmol) in 15 ml of hexane was added 2.4 equivalents of $\text{Co}_2(\text{CO})_8$ (153.3 mg, 0.430 mmol) in hexane. After stirring for 12 h at r.t. the volatiles were removed under vacuum. The residue was dissolved in diethyl ether and hexane, filtered and recrystallized. $^1\text{H-NMR}$ (300 MHz, C_6D_6) δ 7.66 (d, 1H), 7.57 (q, 2H), 7.40 (d, 1H), 6.88 (t, 2H), 6.77 (q, 2H), 1.54 (m, 2H), 1.29 (d, 12H); $^{13}\text{C-NMR}$ (75 MHz, C_6D_6) δ 200.1, 198.9, 140.4, 139.6, 136.2, 134.3, 132.7, 132.4, 129.9, 129.7, 128.2, 127.9, 123.8, 122.2, 108.1, 106.0, 102.7, 99.1, 98.0, 87.0, 76.7, 71.4, 19.3, 18.7, 14.9.

Table 7

Atomic coordinates [$\times 10^4$] and equivalent isotropic displacement parameters [$\text{\AA}^2 \times 10^3$] for compound **4**^a

	<i>x/a</i>	<i>y/b</i>	<i>z/c</i>	<i>U</i> _(eq)
Si	1297(1)	1974(1)	7676(1)	16(1)
C(1)	2198(1)	560(2)	7834(1)	20(1)
C(2)	2785(1)	–385(2)	7916(1)	20(1)
C(3)	3527(1)	–1440(2)	8029(1)	19(1)
C(4)	4336(1)	–1054(2)	8521(1)	19(1)
C(5)	4354(1)	368(2)	8906(1)	21(1)
C(6)	4207(1)	1587(2)	9160(1)	21(1)
C(7)	3941(1)	2968(2)	9403(1)	21(1)
C(8)	3630(1)	4151(2)	9582(1)	20(1)
C(9)	3152(1)	5500(2)	9728(1)	19(1)
C(10)	2263(1)	5715(2)	9326(1)	18(1)
C(11)	1887(1)	4584(2)	8774(1)	19(1)
C(12)	1634(1)	3583(2)	8321(1)	20(1)
C(13)	3474(1)	–2832(2)	7670(1)	22(1)
C(14)	4207(1)	–3817(2)	7775(1)	25(1)
C(15)	5008(1)	–3422(2)	8237(1)	24(1)
C(16)	5072(1)	–2051(2)	8611(1)	22(1)
C(17)	3537(1)	6593(2)	10247(1)	22(1)
C(18)	3060(1)	7897(2)	10365(1)	22(1)
C(19)	2187(1)	8104(2)	9980(1)	22(1)
C(20)	1789(1)	7022(2)	9469(1)	21(1)
C(21)	1253(1)	2460(2)	6512(1)	21(1)
C(22)	159(1)	1240(2)	8072(1)	17(1)
C(23)	975(1)	1124(2)	5968(1)	27(1)
C(24)	2185(1)	3105(2)	6218(1)	34(1)
C(25)	–663(1)	2297(2)	7928(1)	26(1)
C(26)	250(1)	819(2)	9017(1)	24(1)

^a *U*_(eq) is defined as one third of the trace of the orthogonalized *U*_{*ij*} tensor.

Table 8

Atomic coordinates [$\times 10^4$] and equivalent isotropic displacement parameters [$\text{\AA}^2 \times 10^3$] for compound **5**^a

	<i>x/a</i>	<i>y/b</i>	<i>z/c</i>	<i>U</i> _(eq)
Si	−80(1)	1258(1)	1127(1)	21(1)
C(1)	1920(4)	574(1)	1501(2)	25(1)
C(2)	3127(4)	99(1)	1731(1)	24(1)
C(3)	4450(4)	−481(1)	2025(2)	24(1)
C(4)	3677(4)	−797(1)	2808(2)	26(1)
C(5)	1713(5)	−504(1)	3296(2)	28(1)
C(6)	51(5)	−176(1)	3600(2)	29(1)
C(7)	−1832(5)	242(1)	3855(2)	28(1)
C(8)	−3432(5)	644(1)	3991(2)	28(1)
C(9)	−5203(4)	1170(1)	4038(2)	25(1)
C(10)	−5218(4)	1651(1)	3361(2)	24(1)
C(11)	−3517(4)	1582(1)	2643(2)	23(1)
C(12)	−2080(4)	1490(1)	2049(2)	24(1)
C(13)	6425(4)	−746(1)	1554(2)	28(1)
C(14)	7605(5)	−1320(1)	1830(2)	33(1)
C(15)	6810(5)	−1639(1)	2583(2)	34(1)
C(16)	4873(5)	−1381(1)	3070(2)	33(1)
C(17)	−6909(5)	1223(1)	4723(2)	32(1)
C(18)	−8595(5)	1742(1)	4743(2)	34(1)
C(19)	−8607(5)	2212(1)	4083(2)	33(1)
C(20)	−6938(4)	2168(1)	3397(2)	28(1)
C(21)	−2089(5)	966(1)	195(2)	30(1)
C(22)	1856(5)	1969(1)	777(2)	29(1)

^a *U*_(eq) is defined as one third of the trace of the orthogonalized *U*_{ij} tensor.

Table 9

Atomic coordinates [$\times 10^4$] and equivalent isotropic displacement parameters [$\text{\AA}^2 \times 10^3$] for **3**^a

	<i>x/a</i>	<i>y/b</i>	<i>z/c</i>	<i>U</i> _(eq)
C(1)	−437(4)	8258(3)	2256(3)	42(1)
C(2)	543(3)	7861(3)	3450(3)	33(1)
C(3)	1736(3)	7434(3)	4870(3)	29(1)
C(4)	1165(4)	6544(3)	6730(3)	37(1)
C(5)	2328(4)	6147(3)	8093(3)	42(1)
C(6)	4064(4)	6636(3)	7640(3)	38(1)
C(7)	4677(3)	7507(3)	5801(3)	33(1)
C(8)	3522(3)	7917(3)	4405(3)	27(1)
C(9)	4143(3)	8824(3)	2505(3)	28(1)
C(10)	4683(3)	9580(3)	909(3)	28(1)

^a *U*_(eq) is defined as one third of the trace of the orthogonalized *U*_{ij} tensor.

2.3. Crystal structure determinations

X-ray crystallographic data were collected using graphite monochromated Mo K α radiation ($\lambda = 0.710$ 73 Å) on a Syntex P2₁ diffractometer updated to a Siemens R3 *m/v* and equipped with a Molecular Structure Corp. low temperature device. X-ray data were collected using ω scans. The cell dimensions were refined with intensity data from $20^\circ \leq 2\theta \leq 30^\circ$. Systematic absences are consistent with the space groups cho-

sen. The structures were solved by direct methods [28,29]. Hydrogen atoms were calculated and refined using a riding model. Atom positions resulting from

Table 10

Atomic coordinates [$\times 10^4$] and equivalent isotropic displacement parameters [$\text{\AA}^2 \times 10^3$] for **7**^a

	<i>x/a</i>	<i>y/b</i>	<i>z/c</i>	<i>U</i> _(eq)
Si(1)	3412(1)	−1499(1)	1075(1)	20(1)
Si(2)	1811(1)	1198(1)	4189(1)	19(1)
C(1)	4103(2)	−1307(3)	1872(2)	24(1)
C(2)	4520(2)	−1345(3)	2425(2)	23(1)
C(3)	5004(2)	−1519(3)	3095(2)	22(1)
C(4)	5094(2)	−686(3)	3668(2)	22(1)
C(5)	4730(2)	381(3)	3596(2)	24(1)
C(6)	4437(2)	1298(4)	3561(2)	26(1)
C(7)	4119(2)	2365(3)	3528(2)	25(1)
C(8)	3838(2)	3287(3)	3499(2)	26(1)
C(9)	3489(2)	4382(3)	3442(2)	24(1)
C(10)	2827(2)	4437(3)	3594(2)	22(1)
C(11)	2519(2)	3404(3)	3823(2)	21(1)
C(12)	2259(2)	2526(3)	4003(2)	20(1)
C(13)	1217(2)	917(3)	3321(2)	23(1)
C(14)	816(2)	932(3)	2755(2)	20(1)
C(15)	339(2)	1134(3)	2086(2)	21(1)
C(16)	190(2)	315(3)	1516(2)	20(1)
C(17)	521(2)	−798(3)	1569(2)	23(1)
C(18)	788(2)	−1734(3)	1586(2)	24(1)
C(19)	1111(2)	−2794(3)	1617(2)	24(1)
C(20)	1400(2)	−3707(3)	1648(2)	23(1)
C(21)	1762(2)	−4792(3)	1693(2)	21(1)
C(22)	2430(2)	−4825(3)	1566(2)	18(1)
C(23)	2752(2)	−3778(3)	1381(2)	19(1)
C(24)	3024(2)	−2893(3)	1246(2)	20(1)
C(25)	5374(2)	−2551(3)	3192(2)	29(1)
C(26)	5822(2)	−2772(3)	3837(2)	33(1)
C(27)	5912(2)	−1966(4)	4402(2)	32(1)
C(28)	5552(2)	−929(3)	4319(2)	27(1)
C(29)	3784(2)	5391(3)	3222(2)	30(1)
C(30)	3432(2)	6428(3)	3145(2)	33(1)
C(31)	2775(2)	6477(3)	3277(2)	28(1)
C(32)	2475(2)	5496(3)	3497(2)	25(1)
C(33)	17(2)	2227(3)	2007(2)	24(1)
C(34)	−429(2)	2506(4)	1374(2)	33(1)
C(35)	−577(2)	1699(3)	816(2)	33(1)
C(36)	−276(2)	614(3)	885(2)	28(1)
C(37)	1468(2)	−5822(3)	1890(2)	26(1)
C(38)	1827(2)	−6862(3)	1962(2)	27(1)
C(39)	2483(2)	−6880(3)	1831(2)	28(1)
C(40)	2782(2)	−5882(3)	1633(2)	22(1)
C(41)	2745(2)	−362(3)	1056(2)	25(1)
C(42)	3761(2)	−1575(3)	211(2)	21(1)
C(43)	1309(2)	1517(3)	4917(2)	23(1)
C(44)	2436(2)	−17(3)	4397(2)	22(1)
C(45)	2108(2)	−689(3)	498(2)	34(1)
C(46)	2568(2)	−193(3)	1820(2)	36(2)
C(47)	4267(2)	−599(4)	172(2)	44(2)
C(48)	4081(2)	−2758(3)	104(2)	39(2)
C(49)	1025(2)	2756(3)	4855(3)	50(2)
C(50)	738(2)	649(3)	4938(2)	38(2)
C(51)	2102(2)	−1204(3)	4468(2)	28(1)
C(52)	2880(2)	−82(3)	3810(2)	38(2)

^a *U*_(eq) is defined as one third of the trace of the orthogonalized *U*_{ij} tensor.

Table 11

Atomic coordinates [$\times 10^4$] and equivalent isotropic displacement parameters [$\text{\AA}^2 \times 10^3$] for **9**^a

	<i>x</i>	<i>y</i>	<i>z</i>	<i>U</i> _(eq)
Co(1)	2623(1)	−2950(1)	4183(1)	30(1)
Co(2)	1970(1)	−3536(1)	5054(1)	32(1)
Co(3)	4017(1)	1578(1)	3657(1)	29(1)
Co(4)	3210(1)	2760(1)	4055(1)	31(1)
Si	1157(1)	−1137(2)	4038(2)	28(1)
O(1A)	2923(4)	−1358(5)	3116(4)	44(2)
O(1B)	4137(4)	−3896(6)	5052(5)	65(2)
O(1C)	1776(4)	−4372(6)	2758(5)	61(2)
O(2A)	1359(4)	−2983(6)	6281(5)	71(3)
O(2B)	3064(4)	−5258(5)	5929(5)	52(2)
O(2C)	690(4)	−4770(5)	3811(4)	47(2)
O(3A)	4548(4)	3158(5)	2766(5)	62(2)
O(3B)	4130(4)	−357(5)	2758(4)	46(2)
O(3C)	5311(4)	1362(5)	5323(5)	48(2)
O(4A)	3515(13)	4711(12)	3319(16)	40(3)
O(4A')	3192(10)	4600(10)	2935(13)	40(3)
O(4B)	1713(4)	3195(5)	3984(4)	51(2)
O(4C)	4333(12)	3272(18)	5744(13)	49(3)
O(4C')	4146(8)	2903(12)	5901(8)	49(3)
C(1)	1943(5)	−2085(7)	4546(6)	27(2)
C(1A)	2810(5)	−1962(7)	3541(7)	39(3)
C(1B)	3553(6)	−3540(8)	4701(7)	48(3)
C(1C)	2100(5)	−3787(8)	3300(7)	38(3)
C(2)	2610(5)	−2269(6)	5205(5)	22(2)
C(2A)	1571(6)	−3234(8)	5795(7)	42(3)
C(2B)	2644(6)	−4587(8)	5603(6)	34(3)
C(2C)	1193(6)	−4278(7)	4270(6)	33(3)
C(3)	3206(5)	−1810(6)	5952(6)	22(2)
C(3A)	4337(5)	2524(7)	3090(6)	32(3)
C(3B)	4090(5)	388(8)	3113(6)	37(3)
C(3C)	4813(5)	1446(7)	4665(7)	37(3)
C(4)	3557(5)	−797(6)	5948(6)	28(2)
C(4A)	3418(16)	3933(17)	3606(17)	34(4)
C(4A')	3182(13)	3911(14)	3370(14)	34(4)
C(4B)	2303(5)	3021(7)	4028(6)	36(3)
C(4C)	3909(14)	3153(23)	5051(15)	35(4)
C(4C')	3786(9)	2866(15)	5176(11)	35(4)
C(5)	3316(5)	−187(7)	5167(6)	30(2)
C(6)	3222(5)	416(7)	4591(6)	28(2)
C(7)	3209(5)	1179(6)	4001(7)	29(2)
C(8)	2912(5)	1612(6)	3215(6)	24(2)
C(9)	2285(5)	1515(7)	2371(6)	29(2)
C(10)	1658(5)	874(7)	2198(6)	27(2)
C(11)	1553(5)	258(7)	2849(6)	28(2)
C(12)	1400(5)	−288(7)	3319(6)	29(2)
C(13)	3479(5)	−2356(7)	6733(6)	34(2)
C(14)	4046(5)	−1915(7)	7451(6)	33(2)
C(15)	4358(5)	−918(7)	7439(6)	31(2)
C(16)	4119(5)	−384(7)	6681(6)	24(2)
C(17)	2338(5)	2130(7)	1717(6)	36(2)
C(18)	1761(5)	2087(7)	904(7)	36(2)
C(19)	1136(5)	1458(8)	759(6)	42(3)
C(20)	1087(5)	837(7)	1381(6)	31(2)
C(21)	268(5)	−1886(7)	3387(6)	32(2)
C(22)	263(5)	−2404(8)	2579(6)	51(3)
C(23)	−459(5)	−1261(7)	3145(7)	47(3)
C(24)	1012(5)	−272(6)	4845(6)	27(2)
C(25)	644(5)	810(7)	4448(6)	39(3)
C(26)	1714(5)	−71(7)	5649(6)	48(3)

^a $U_{\text{(eq)}}$ is defined as one third of the trace of the orthogonalized U_{ij} tensor.

least-squares refinement [30] for compounds **3**, **4**, **5**, **7** and **9** are listed in Tables 7–11.

3. Conclusion

In conclusion, several new silicon diacetylenic heterocyclines have been synthesized and structurally characterized. We attempted to induce solid state 1,4-addition polymerizations on these silicon heterocyclines. Compounds **3** and **5** were irradiated for several days turning a dark color. However, polymerization occurred only on the surface and not throughout the bulk of **3** and **5**. The heterocyclines **3**, **4**, **5** and **6** were annealed but due to poor solubility the products have not yet been characterized.

Acknowledgements

We would like to thank the National Science Foundation for financial support and Zhengjie Pi for acquiring the $^1\text{H}\{^{29}\text{Si}\}$ NMR data for compound **6**. Supporting Information Available: tables of anisotropic thermal parameters, bond lengths and angles, and hydrogen parameters for compounds **4**, **5**, **6**, **7** and **9** are available from the authors.

References

- [1] G.Z. Wegner, *Naturforsch* 24b (1969) 824.
- [2] W.D. Huntsman, in: S. Patai, Z. Rappoport (Eds.), *The chemistry of functional groups, supplement C*, John Wiley, NY, 1983, pp. 917–980.
- [3] G.M. Carter, Y.J. Chen, M.F. Rubner, D.J. Sandman, M.K. Thakur, S.K. Tripathy, in: D.S. Chemla, J. Zyss (Eds.), *Nonlinear optical properties of organic molecules and crystals*, vol. 2, Academic, NY, 1987, pp. 85–120.
- [4] R.R. Chance, M.L. Shand, C. Hogg, R. Sillbey, *Phys. Rev* 22b (1980) 3540.
- [5] D. Moses, S. Phillips, M. Sinclair, A.J. Heeger, in: A.J. Heeger, J. Orenstein, D.R. Ulrich (Eds.), *Nonlinear optical properties of polymers*, North-Holland Press, NY, 1988, pp. 195–201.
- [6] M.S. Paley, D.O. Frazier, H. Abeledyem, S.P. McManus, S.E. Zutaut, *J. Am. Chem. Soc.* 114 (1992) 3247.
- [7] M. Jalali-Heravi, S.E. Zutaut, S.P. McManus, *Polym. Prepr.* 32 (1991) 78.
- [8] (a) L. Guo, J.D. Bradshaw, C.A. Tessier, W.J. Youngs, *Organometallics* 14 (1995) 586. (b) L. Guo, J.D. Bradshaw, D.B. McConville, C.A. Tessier, W.J. Youngs, *Organometallics* 16 (1997) 1685.
- [9] L. Guo, J.D. Bradshaw, C.A. Tessier, W.J. Youngs, *J. Chem. Soc. Chem. Comm.* 3 (1994) 243.
- [10] R.J.P. Corriu, N. Devylder, C. Guérin, B. Henner, A. Jean, *Organometallics* 13 (1994) 3194 and references therein.
- [11] J.L. Bréfort, R.J.P. Corriu, P. Gerbier, C. Guérin, B.J.L. Henner, A. Jean, T. Kuhlmann, F. Garnier, A. Yassar, *Organometallics* 11 (1992) 2500.
- [12] K.P. Baldwin, A.J. Matzger, D.A. Scheiman, C.A. Tessier, K.P.C. Vollhardt, W.J. Youngs, *Synlett* 12 (1995) 1215.

- [13] R. Bortolin, S.S.D. Brown, B. Parbhoo, *Inorg. Chim. Acta* 158 (1989) 137.
- [14] E. Hengge, A. Baumegger, *J. Organomet. Chem.* 369 (1989) C39.
- [15] L.T. Scott, M.J. Cooney, C. Otte, C. Puls, T. Haumann, R. Boese, P.J. Carroll, A.B. Smith III, A. Meijere, *J. Am. Chem. Soc.* 116 (1994) 10275.
- [16] L.T. Scott, M.J. Cooney, D. Johnels, *J. Am. Chem. Soc.* 112 (1990) 4054.
- [17] T. Matsuoka, T. Negi, T. Otsubo, Y. Sakata, S. Misumi, *Bull. Chem. Soc. Jpn.* 45 (1972) 1825.
- [18] L. Guo, Ph. D. Dissertation, The University of Akron, 1996.
- [19] K.H. Pannell, G.M. Crawford, *Coord. Chem.* 2 (1973) 251.
- [20] P. Magnus, D.P. Becker, *J. Chem. Soc. Chem. Commun.* 10 (1985) 640.
- [21] F.R. Fronczek, M.S. Erickson, *J. Chem. Cryst.* 25 (1995) 737.
- [22] R.H. Baughman, *J. Polym. Sci. Polym. Phys. Ed.* 12 (1974) 1511.
- [23] G. Wegner, in: H.J. Keller (Ed.), *Chemistry and physics of one-dimensional metals*, NY: Plenum, 1976, pp. 297–314.
- [24] W.G. Kofron, L.M. Baclawski, *J. Org. Chem.* 41 (1976) 1879.
- [25] D. Solooki, J.D. Ferrara, D. Malaba, J.D. Bradshaw, C.A. Tessier, W.J. Youngs, *Inorg. Synth.* 31 (1997) 122.
- [26] D.F. Shriver, M.A. Drezdson, *The manipulation of air-sensitive compounds*, 2nd edition, Wiley, NY, 1986, p. 1986.
- [27] A.L. Wayda, P.A. Bianconi, in: A.L. Wayda, M.Y. Darensbourg (Eds.), *Experimental organometallic chemistry*, Chapter 3, Application 5, American Chemical Society, Washington, DC, 1987.
- [28] G.M. Sheldrick, *SHELXS86*, *Acta Crystallogr. Sect. A.* 46 (1990) 467.
- [29] *SHELXTL-Plus Vers. 4.03 and 5.03*: Siemens Analytical X-ray Instruments, Madison, WI, 1990 and 1994, respectively.
- [30] G.M. Sheldrick, *SHELXL93*, University of Goettingen, Germany, 1993.